740562

Closed-Form Solution to Rate Equations for an $F + H_2$ Laser Oscillator

Prepared by G. EMANUEL and J. S. WHITTIER
Aerodynamics and Propulsion Research Laboratory

72 APR 15

Laboratory Operations
THE AEROSPACE CORPORATION

Prepared for SPACE AND MISSILE SYSTEMS ORGANIZATION
AIR FORCE SYSTEMS COMMAND
LOS ANGELES AIR FORCE STATION
Los Angeles, California

LABORATORY OPERATIONS

The Laboratory Operations of The Aerospace Corporation is conducting experimental and theoretical investigations necessary for the evaluation and application of scientific advances to new military concepts and systems. Versatility and flexibility have been developed to a high degree by the laboratory personnel in dealing with the many problems encountered in the nation's rapidly developing space and missile systems. Expertise in the latest scientific developments is vital to the accomplishment of tasks related to these problems. The laboratories that contribute to this research are:

Aerodynamics and Propulsion Research Laboratory: Launch and reentry aerodynamics, heat transfer, reentry physics, propulsion, high-temperature chemistry and chemical kinetics, structural mechanics, flight dynamics, atmospheric pollution, and high-power gas lasers.

Electronics Research Laboratory: Generation, transmission, detection, and processing of electromagnetic radiation in the terrestrial and space environments, with emphasis on the millimeter-wave, infrared, and visible portions of the spectrum; design and fabrication of antennas, complex optical systems, and photolithographic solid-state devices; test and development of practical superconducting detectors and laser devices and technology, including high-power lasers, atmospheric pollution, and biomedical problems.

Materials Sciences Laboratory: Development of new materials; metal matrix composites and new forms of carbon, test and evaluation of graphite and ceramics in reentry, spacecraft materials and components in radiation and high-vacuum environments, application of fracture mechanics to stress corrosion and fatigue-induced fractures in structural metals; effect of nature of material surfaces on lubrication, photosensitization, and catalytic reactions, and development of prosthesis devices.

Plasma Research Laboratory: Reentry physics and nuclear weapons effects, the interaction of antennas with reentry plasma sheaths, experimentation with thermonuclear plasmas, the generation and propagation of plasma waves in the magnetosphere, chemical reactions of vibrationally excited species in rocket plumes, and high-precision laser ranging.

Space Physics Laboratory: Aeronomy, density and composition of the atmosphere at all altitudes, atmospheric reactions and atmospheric optics; pollution of the environment; the sun, earth's resources; meteorological measurements, radiation belts and cosmic rays, and the effects of nuclear explosions, magnetic storms, and solar radiation on the atmosphere.

THE AEROSPACE CORPORATION
El Segundo, California

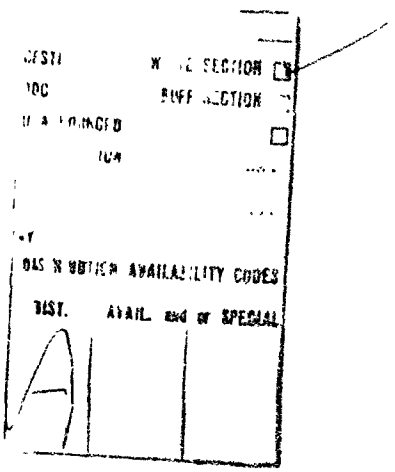

UNCLASSIFIED

Security Classification

DOCUMENT CONTROL DATA - R & D

(Security classification of title, body of abstract and indexing annotation must be entered when the overall report is classified)

1. ORIGINATING ACTIVITY (Corporate author)	2a. REPORT SECURITY CLASSIFICATION
The Aerospace Corporation El Segundo, California	Unclassified
	2b. GROUP

3. REPORT TITLE

Closed-Form Solution to Rate Equations for an $F + H_2$ Laser

4. DESCRIPTIVE NOTES (Type of report and inclusive dates)

5. AUTHOR(S) (First name, middle initial, last name)

George Emanuel and James S. Whittier

6. REPORT DATE	7a. TOTAL NO. OF PAGES	7b. NO. OF REFS
72 APR 15	38	7

8a. CONTRACT OR GRANT NO.	9a. ORIGINATOR'S REPORT NUMBER(S)
F04701-71-C-0172	TR-0172(2754)-1
b. PROJECT NO.	
c	9b. OTHER REPORT NO(S) (Any other numbers that may be assigned this report)
d	SAMSO-TR-72-71

10. DISTRIBUTION STATEMENT

Approved for public release; distribution unlimited

11. SUPPLEMENTARY NOTES	12. SPONSORING MILITARY ACTIVITY
	Space and Missile Systems Organization Air Force Systems Command United States Air Force

13. ABSTRACT

Chemical lasers pumped by the reaction of atomic fluorine with molecular hydrogen emit power from rotation-vibration transitions of excited HF with upper levels as high as v = 3. Collisional processes compete with stimulated emission for the energy of the excited HF. A simplified analysis is presented here for intensity, energy, and chemical efficiency of a class of such lasers. Results are obtained in closed form. A comparison with more exact computer solutions establishes the validity of the analysis despite its simplifications. A comprehensive parametric study examines the relative importance of initial conditions, optical cavity parameters, and rate coefficients for pumping and deactivation reactions.

DD FORM 1473

14.

KEY WORDS

Chemical laser performance
$F + H_2$ kinetics
Rate equations solution

Distribution Statement (Continued)

Abstract (Continued)

Air Force Report No.
SAMSO-TR-72-71

Aerospace Report No.
TR-0172(2754)-1

CLOSED-FORM SOLUTION TO RATE EQUATIONS FOR AN $F + H_2$ LASER OSCILLATOR

Prepared by

G. Emanuel and J. S. Whittier
Aerodynamics and Propulsion Research Laboratory

72 APR 15

Laboratory Operations
THE AEROSPACE CORPORATION

Prepared for

SPACE AND MISSILE SYSTEMS ORGANIZATION
AIR FORCE SYSTEMS COMMAND
LOS ANGELES AIR FORCE STATION
Los Angeles, California

FOREWORD

This report is published by The Aerospace Corporation, El Segundo, California. The research was supported by the Advanced Research Projects Agency of the Department of Defense under U. S. Air Force Space and Missile Systems Organization (SAMSO) Contract F04701-71-C-0172.

This report, which documents research carried out from September 1970 through March 1971, was submitted on 10 November 1971 to Captain Richard K. Strome, SYAE, for review and approval.

Approved

W. R. Warren, Jr., Director
Aerodynamics and Propulsion
Research Laboratory

Publication of this report does not constitute Air Force approval of the report's findings or conclusions. It is published only for the exchange and stimulation of ideas.

Richard K. Strome
Richard K. Strome
Captain, United States Air Force
Project Officer

ABSTRACT

Chemical lasers pumped by the reaction of atomic fluorine with molecular hydrogen emit power from rotation-vibration transitions of excited HF with upper levels as high as v = 3. Collisional processes compete with stimulated emission for the energy of the excited HF. A simplified analysis is presented here for intensity, energy, and chemical efficiency of a class of such lasers. Results are obtained in closed form. A comparison with more exact computer solutions establishes the validity of the analysis despite its simplifications. A comprehensive parametric study examines the relative importance of initial conditions, optical cavity parameters, and rate coefficients for pumping and deactivation reactions.

CONTENTS

TABLES

FIGURES

NOMENCLATURE

$a(v)$	vibrational-level distribution constants
A	cross-sectional area of the flow (cw case)
A_1, A_2	defined by Eqs. (4)
c	speed of light in vacuum
d_i	reaction rate parameters
E	cumulative pulse energy per unit volume of gas
g	gain coefficient
h	Planck's constant
I	intensity
J	rotational quantum number
k	chemical rate coefficient
$\bar{k}$	ratio of chemical rate coefficient to that for $F + H_2$ reaction
L	length of active medium between the mirrors
m_i	parameters that depend on $J\Theta_r/T$
$\mathcal{M}$	matrix element of the electric dipole moment
$n(v)$	mole-mass ratio of vibrational level v
n_i	mole-mass ratio of species i
n_{tot}	overall mole-mass ratio of lasing species
N_A	Avogadro's number
p	pressure
P	cumulative output power (cw case)
r_1, r_2	mirror reflectivities
R	universal gas constant 1.987 cal/mole-°K

t	time
T	temperature
u	flow speed (cw case)
v	vibrational quantum number
v_f	highest vibrational level considered
W	molecular weight of excited species
x	distance in the flow direction (cw case)
α	defined by Eq. (32)
δ	Θ_r/T
η	chemical efficiency
Θ_r	characteristic rotational temperature
κ_1	$(n_F/n_{H_2})_0$
κ_2	$(n_{HF}/n_F)_0$
ξ	extent of reaction
ρ	density
σ	symmetry factor
τ	characteristic time for pumping reaction
$\chi_{ch}(v)$	net rate of production of $n(v)$ by chemical reaction
χ_{rad}	overall rate of stimulated emission, Eq. (3)
$\chi_{rad}(v)$	rate of production of $n(v)$ by lasing from $v + 1$ to v
ω	wavenumber of lasing transition

Subscripts

c	designates lasing cutoff
0	designates threshold or initial condition

I. INTRODUCTION

This paper presents a closed-form analytical description of an HF chemical laser pumped by the reaction of atomic fluorine with molecular hydrogen. Simultaneous effects of laser power extraction, chemical pumping, and chemical deactivation are considered within the idealization of volume uniformity of these processes. Hence, the results are most applicable to lasers having premixed reactants, as in the pulsed laser analysis of Airey.[1] The analysis is also applicable to a cw laser when the reactants are rapidly mixed and the cavity is a Fabry-Perot resonator. Modifications to the pulse analysis for description of cw operation are given in an appendix.

One of the authors[2] has developed a comprehensive computer program that calculates the performance of a chemical laser by numerically integrating a system of nonlinear equations. To complement such computations, we have undertaken the present investigation with the objective of deriving approximate closed-form expressions for intensity, energy, and chemical efficiency. Features of the present simplified model and the computer model are summarized in Table I and discussed in the following paragraphs.

Section II presents the formulation of an analytical model for a multi-level laser. We assume that from lasing threshold to cutoff there is simultaneous lasing between all pairs of adjacent vibrational levels. This assumption allows the use of gain expressions to establish the relative populations of different vibrational levels. For tractability, we restrict our attention to a Doppler-broadened gain profile.

Table I. Comparison of Theoretical Models

Feature	Present Analysis	Computer Model
Lasing threshold	Occurs simultaneously for all bands at t = 0.	Occurs when Eq. (7) is first satisfied. Individual bands treated separately.
Lasing cutoff	Occurs simultaneously for all bands.	Individual bands treated separately.
Line broadening	Doppler.	Simultaneous Doppler and collisional.
J	Lasing on single J for whole pulse and for all vibrational bands.	Lasing on maximum gain transition for each band; calculates J's as part of solution.
Rotational population distribution	Boltzmann at translational temperature.	Boltzmann at translational temperature.
Temperature	Constant.	Calculated as part of solution.
Vibrational energy levels	Harmonic.	Anharmonic.
Reactions modelled	See Table II; most backward rates neglected.	Forward and backward rates for all reactions of Table II. Also other VT and VV and recombination-dissociation processes.

Section III presents the simplified chemical kinetic model that is employed in the analysis. Guided by results of computer calculations[3,4] employing a more comprehensive kinetic model, we select predominant reactions and treat most of these as unidirectional in their dominant direction. For tractability, a constant temperature is assumed. Consequently, the analysis is most useful for mixtures containing large amounts of inert diluent.

The multi-level model is specialized to the case of an HF laser in which pumping is furnished by the reaction

$$F + H_2 \rightarrow HF(v) + H, \qquad v = 0, 1, 2, 3$$

Expressions are derived that show the effects of initial composition, temperature, and optical cavity output coupling on laser performance. Interestingly, the results are independent of rate coefficients for VV collisions between HF molecules.

Selected cases are compared with results obtained with the more comprehensive computer model. The agreement is seen to be good. The effects of the parameters are illustrated by consideration of numerical examples.

II. FORMULATION OF THE MULTI-LEVEL LASER MODEL

Rate equations for a chemically reacting system in which lasing may occur between adjacent vibrational levels are

$$\left.\begin{aligned} \rho\frac{dn(0)}{dt} &= \chi_{ch}(0) + \chi_{rad}(0) \\ \rho\frac{dn(1)}{dt} &= \chi_{ch}(1) + \chi_{rad}(1) - \chi_{rad}(0) \\ &\cdots \\ \rho\frac{dn(v_f)}{dt} &= \chi_{ch}(v_f) - \chi_{rad}(v_f - 1) \end{aligned}\right\} \quad (1)$$

Here $n(v)$ is the number of moles in vibrational level v per unit mass, ρ is density, $\chi_{ch}(v)$ is net production of $n(v)$ by chemical reactions, $\chi_{rad}(v)$ is production of $n(v)$ by lasing from $v + 1 \rightarrow v$, and v_f is the highest vibrational level considered. In the absence of lasing between a pair of levels, the appropriate $\chi_{rad}(v)$ is zero. We assume that lasing is, in fact, occurring between all the levels. All χ_{rad}'s are thus positive during a time interval (t_0, t_c), where t_0 is a threshold time and t_c is the lasing cutoff time. Justification for this approximation may be found in discussions of computer modeling of HF lasers.[3,4] Study of cw and pulsed lasers pumped by the $F + H_2$ reaction shows that the bulk of the laser energy extraction (>90 %) occurs when there is simultaneous lasing on the $v = 1 \rightarrow 0$, $2 \rightarrow 1$, and $3 \rightarrow 2$ bands.

Equations (1) are easily inverted for the $\chi_{rad}(v)$

$$\left.\begin{aligned}
\chi_{rad}(0) &= \rho\frac{d}{dt}n(0) - \chi_{ch}(0) \\
\chi_{rad}(1) &= \rho\frac{d}{dt}[\,n(0) + n(1)] - [\,\chi_{ch}(0) + \chi_{ch}(1)] \\
&\cdots \\
\chi_{rad}(v_f - 1) &= \rho\frac{d}{dt}[\,n(0) + \cdots + n(v_f - 1)] \\
&\quad - [\,\chi_{ch}(0) + \cdots + \chi_{ch}(v_f - 1)]
\end{aligned}\right\} \qquad (2)$$

The last of Eqs. (1) is not needed in this inversion. Summation of Eqs. (2) yields

$$\chi_{rad} \equiv \sum_{v=0}^{v_f-1} \chi_{rad}(v) = A_1 - A_2 \qquad (3)$$

where

$$A_1 \equiv \rho \sum_{v=0}^{v_f-1} (v_f - v)\frac{dn(v)}{dt} \qquad (4a)$$

$$A_2 \equiv \sum_{v=0}^{v_f-1} (v_f - v)\chi_{ch}(v) \qquad (4b)$$

The quantity χ_{rad} is central to the analysis, since it is used in the determination of pulse energy, intensity, and efficiency.

If we assume that all lasing transitions have the same wavenumber ω, then the cumulative pulse energy per unit volume of gas E(t) is simply[5]

$$E(t) = hcN_A\omega\int_{t_0}^{t}\chi_{rad}\,dt = 11.96\,\omega\int_{t_0}^{t}\chi_{rad}\,dt \qquad (5)$$

Here E is in joule/cm^3 and ω is in cm^{-1}.

We later use the F + H_2 reaction for pumping. Available chemical energy from this reaction is 1.40×10^5 J/mole of F atoms. With the notation $(\ )_0$ for an initial value, the chemical efficiency η is, in percent,

$$\eta = \frac{11.96 \times 10^2\omega}{1.4 \times 10^5\,\rho(n_F)_0}\int_{t_0}^{t_c}\chi_{rad}\,dt \qquad (6)$$

where n_F is the mole-mass ratio of atomic fluorine.

For calculation of χ_{rad}, the n(v)'s that occur during lasing may be determined by consideration of the gain required for lasing in a specified optical cavity. For a cavity with mirror reflectivities r_1 and r_2, the required gain per unit length g is controlled by[6]

$$r_1 r_2\, e^{2Lg(v,J)} = 1, \qquad v = 0, \cdots, v_f - 1 \qquad (7)$$

where L is the length of active medium between the mirrors, and, for simplicity, scattering and diffraction losses are not included. If rotational

equilibrium at the translational temperature is assumed, the gain per unit length at line center of a Doppler-broadened P-branch transition is given by[5]

$$g(v, J) = g_r J\, e^{-(J^2-J)\delta}[n(v+1) - n(v)\, e^{-2J\delta}] \tag{8}$$

Here the reference gain g_r and temperature ratio δ are defined by

$$g_r \equiv 2.74 \times 10^{47}\, \sigma \Theta_r W^{1/2} T^{-3/2} \rho\, |\mathcal{M}|^2, \qquad \delta \equiv \Theta_r / T \tag{9}$$

where σ is a symmetry factor, Θ_r is the characteristic rotational temperature, W is the molecular weight of the lasing species, T is the translational temperature, and $\mathcal{M}$ is the matrix element of the electric dipole moment.

The output intensity in W/cm^2 is given by[5]

$$I = 11.96\, \omega \left[1 - (r_1 r_2)^{1/2}\right] \chi_{rad} / g \tag{10}$$

We assume that in the set of Eqs. (8) the lower-level rotational quantum number J is the same for all lasing transitions. This value for J will later be chosen to maximize the efficiency. We were led to this simplification by previous analysis[5] and numerical solutions [3, 4] in which most of the power (>75 %) emanates from only two or three transitions for each $v + 1 \rightarrow v$ band. The J's of these dominant transitions do not vary much with v. The use here of a single J for all levels and for the entire pulse duration permits a simple and reasonably accurate total energy prediction. In consequence, however, we

sacrifice detailed prediction of spectral content and obtain only a single dominant J.

With this dominant J assumption, Eqs. (8), with their lefthand sides replaced by the g satisfying Eq. (7), can be solved for the n(v)'s. After manipulation, the result is

$$n(v) = \frac{1 - e^{-2J\delta}}{1 - e^{-2J\delta(v_f+1)}} e^{-2J\delta v} n_{tot} + \frac{g}{g_r} \frac{e^{(J^2-J)\delta}}{J}$$

$$\times \left[\frac{(1 - e^{-2J\delta v})\left[1 - e^{-2J\delta(v_f+1)}\right] - v_f e^{-2J\delta v}(1 - e^{-2J\delta}) + e^{-2J\delta(v+1)}\left(1 - e^{-2J\delta v_f}\right)}{(1 - e^{-2J\delta})\left[1 - e^{-2J\delta(v_f+1)}\right]} \right], \qquad (11)$$

$$v = 0, 1, \cdots, v_f$$

where n_{tot} is the total mole-mass ratio of the lasing species, i.e.

$$n_{tot} = \sum_{v=0}^{v_f} n(v)$$

Equation (11) is valid during lasing but not before threshold or after cutoff. During lasing, g, J, and δ are constant, thus

$$\frac{d}{dt}n(v) = \frac{1 - e^{-2J\delta}}{1 - e^{-2J\delta(v_f+1)}} e^{-2J\delta v} \frac{d}{dt}n_{tot}, \qquad v = 0, 1, \cdots, v_f \qquad (12)$$

III. CHEMICAL KINETICS

Dominant kinetic processes involved in the class of HF lasers pumped by the $F + H_2$ reaction are now described. For each reaction we define vibrational-level distribution constants a(v) such that

$$\sum_{v=0}^{v_f} a(v) = 1 \tag{13}$$

For example, the forward rate coefficient k(v) for the pumping reaction is written as k(v) = a(v)k(T), where k(T) is the overall forward rate coefficient. Our choice of reactions, overall rate coefficients, and distribution constants is shown in Table II. This choice is based on analysis of computer solutions for flow and pulsed HF lasers.[3,4] Numerical values for the rates and distribution constants are taken from Ref. 4.

Disregarding backward rates for Reacts. (R-1)-(R-4) is legitimate during lasing but, of course, is incorrect later when equilibrium is approached.

Reactions (R-2) and (R-4) are the dominant VT processes. For React. (R-2) we use a numerical fit to rate data of Airey and Fried.[7] The distribution constants in Reacts. (R-2) and (R-4) are based on a harmonic oscillator approximation.

Reactions (R-3), (R-5), and (R-6) represent dominant VV processes. In application of React. (R-3) we shall use, in the lefthand side, total concentration of H_2 rather than $H_2(0)$. The error incurred is small. Backward and

Table II. Chemical Model for the F + H_2 Laser

Reaction Number	Reaction	Overall Rate Coefficients[a]		Distribution Constants a(v)			
		Forward	Backward	v = 0	1	2	3
R-1	$F + H_2 \rightleftharpoons HF(v) + H$	$k = 1.62 \times 10^{14} e^{-1600/RT}$	$k_b = 0$	0.056	0.111	0.555	0.278
R-2	$HF(v) + HF \rightleftharpoons HF(v-1) + HF$	$k_{HF} = 6 \times 10^{16} T^{-1.43}$	$k_b = 0$	0	0.167	0.333	0.500
R-3	$HF(v) + H_2(0) \rightleftharpoons HF(v-1) + H_2(1)$	$k_{H_2} = 8.3 \times 10^{5} T^{2.2} e^{-562/RT}$	$k_b = 0$	0	0.965	0.035	0
R-4	$HF(v) + F \rightleftharpoons HF(v-1) + F$	$k_F = 5.4 \times 10^{9} T^{1.3}$	$k_b = 0$	0	0.167	0.333	0.500
R-5	$2HF(v) \rightleftharpoons HF(v-1) + HF(v+1)$	$k_{fHF}(T)$	$k_b = 0$	c	$a_f(1)$	$a_f(2)$	0
R-6	$2HF(v) \rightleftharpoons HF(v-1) + HF(v+1)$	$k_f = 0$	$k_{bHF}(T)$	0	$a_b(1)$	$a_b(2)$	0

[a]All rate coefficients are in cm^3/mole-sec, and R = 1.987 cal/mole-°K.

forward reactions for HF – HF VV's are comparable in magnitude. Therefore, we include the forward reactions as React. (R-5) and the backward reactions as React. (R-6). Nonzero rate and distribution constants for Reacts. (R-5) and (R-6) are given only symbolically in Table II. Later these symbols drop out of the analysis. No VV or VT processes that produce HF(v) with $v > v_f$ are included. These processes are weak.

A process not included in Table II is VT deactivation of HF by the diluent. Such processes[4] have rate coefficients several thousand times smaller than those of React. (R-2), and, unless the diluent concentration is inordinately large, they may be disregarded. As a consequence, the type of diluent and its concentration, providing it is sufficient for the isothermal approximation to apply, do not enter into the analysis.

On the basis of the reactions in Table II we can write $\chi_{ch}(v)$ as

$$\begin{aligned}\chi_{ch}(v) = \rho^2\Big\{ & a(v)k n_F n_{H_2} + k_{HF} n_{HF}\left[a_{HF}(v+1)n(v+1) - a_{HF}(v)n(v)\right] \\ & + k_F n_F\left[a_F(v+1)n(v+1) - a_F(v)n(v)\right] \\ & + k_{H_2} n_{H_2}\left[a_{H_2}(v+1)n(v+1) - a_{H_2}(v)n(v)\right] \\ & + k_{fHF}\left[a_f(v+1)n^2(v+1) - 2a_f(v)n^2(v) + a_f(v-1)n^2(v-1)\right] \\ & + k_{bHF}\left[-a_b(v+1)n(v+2)n(v) + 2a_b(v)n(v+1)n(v-1)\right. \\ & \left. - a_b(v-1)n(v)n(v-2)\right]\Big\} \end{aligned} \tag{14}$$

where a(-1) is zero, and v = 0, 1, 2.

In addition to the reactions, the n_i satisfy atom conservation relations

$$n_H + n_{HF} + 2n_{H_2} = \left(n_H + n_{HF} + 2n_{H_2}\right)_0, \qquad n_F + n_{HF} = (n_F + n_{HF})_0 \tag{15}$$

where $n_{HF} = n_{tot}$.

IV. ANALYSIS

We analyze an idealized situation in which, at t = 0, a homogeneous mixture with reactant composition $(n_H)_0 = 0$, $(n_F)_0$, $(n_{H_2})_0$, and $(n_{HF})_0$ begins to react in accord with the kinetic model of Section III. Assuming that lasing threshold is reached immediately, i.e., that $t_0 = 0$, we determine the time-dependence of the reaction and then calculate intensity, shutoff time, energy, and efficiency.

The composition of F and H changes through React. (R-1) with rate equations

$$\frac{d}{dt} n_F = -\frac{d}{dt} n_H = -k\rho n_F n_{H_2} \tag{16}$$

We thus have

$$n_F + n_H = (n_F + n_H)_0 \tag{17}$$

Use of Eqs. (15) and (17) in (16) gives

$$\frac{d}{dt} n_F = -k\rho n_F \left[n_F + (n_{H_2} - n_F)_0 \right] \tag{18}$$

which integrates to

$$\frac{n_F}{(n_F)_0} = \frac{(1 - \kappa_1)\, e^{-t/\tau}}{1 - \kappa_1\, e^{-t/\tau}} \tag{19}$$

where

$$\kappa_1 \equiv \left(\frac{n_F}{n_{H_2}}\right)_0, \qquad \tau^{-1} \equiv k\rho\left(n_{H_2} - n_F\right)_0 \tag{20}$$

When $\kappa_1 = 1$, solution (19) is indeterminate, and the appropriate form is

$$\frac{n_F}{(n_F)_0} = \left[1 + k\rho(n_F)_0 t\right]^{-1}, \qquad \kappa_1 = 1 \tag{21}$$

The time-dependent composition can be expressed in terms of a single variable, the extent of reaction, defined by

$$\xi = \frac{n_{HF} - (n_{HF})_0}{(n_F)_0} \tag{22}$$

From Eqs. (15), (17), and (22) it can be established that

$$\left.\begin{aligned} n_{HF} &= (n_F)_0 \xi + (n_{HF})_0 \\ n_F &= -(n_F)_0 \xi + (n_F)_0 \\ n_H &= (n_F)_0 \xi + (n_H)_0 \\ n_{H_2} &= -(n_F)_0 \xi + (n_{H_2})_0 \end{aligned}\right\} \tag{23}$$

and use of these in (19) gives

$$\xi = \frac{1 - e^{-t/\tau}}{1 - \kappa_1 e^{-t/\tau}} \tag{24}$$

We now turn to a derivation of χ_{rad}. Use of expression (4a) for A_1, incorporation of Eq. (12) with $n_{tot} = n_{HF}$ and $v_f = 3$, and finally use of Eq. (23) yields

$$A_1 = m_1 \rho (n_F)_0 \frac{d\xi}{dt} \tag{25}$$

where the function m_1, which is plotted in Fig. 1, is given by

$$m_1 = \frac{3 + 2e^{-2J\delta} + e^{-4J\delta}}{\left(1 + e^{-2J\delta}\right)\left(1 + e^{-4J\delta}\right)} \tag{26}$$

Differentiation of Eq. (24) and combination with Eq. (25) gives

$$A_1 = m_1 k \rho^2 \left(n_F n_{H_2}\right)_0 \left(1 - \xi\right)\left(1 - \kappa_1 \xi\right) \tag{27}$$

Substitution of Eq. (14) into Eq. (4b) gives A_2. For brevity we enter numerical values for the a(v)'s to obtain

$$A_2 = \rho^2 \Big\{ 0.945\, k n_F n_{H_2} + \frac{1}{6}\left(k_{HF} n_{HF} + k_F n_F\right)\left[n(1) + 2n(2) + 3n(3)\right] + k_{H_2} n_{H_2}\left[0.965\, n(1) + 0.035\, n(2)\right] \Big\} \tag{28}$$

The HF – HF VV terms from Reacts. (R-5) and (R-6) have cancelled as a result of the assumptions of equal spacing for all vibrational energy levels and simultaneous lasing on all bands. In computer modeling,[3,4] where anharmonic spacing is accounted for, these VV's have a very small effect on total power.

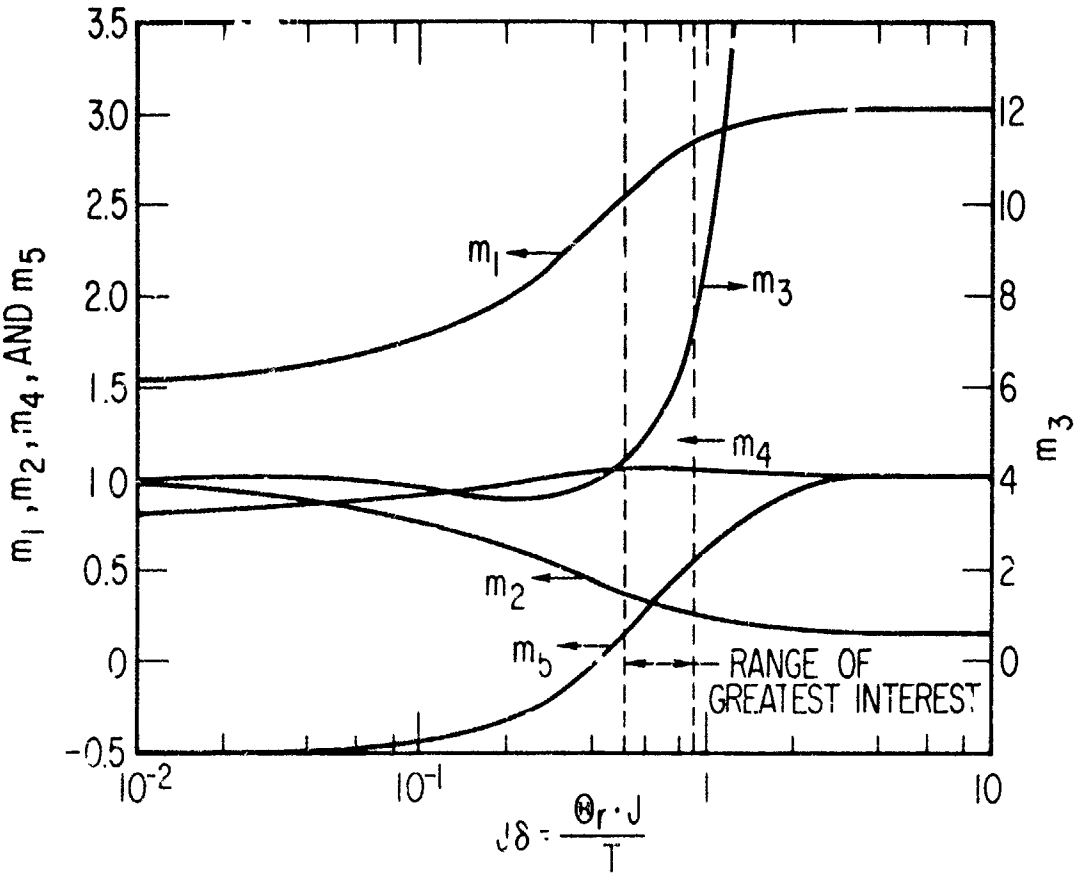

Figure 1. Parameters m_i vs $J\Theta_r/T$
(See Eqs. 26 and 30.)

We further simplify A_2 by setting $0.945 \simeq 1$ and $0.965\, n(1) + 0.035\, n(2) \simeq n(1)$. Into this A_2 we substitute Eq. (11) to obtain

$$A_2 = \rho^2 \left\{ k n_F n_{H_2} + \frac{n_{HF}}{m_3} \left[m_2 (k_{HF} n_{HF} + k_F n_F) + k_{H_2} n_{H_2} \right] \right.$$
$$\left. + \frac{g}{g_r} \frac{e^{(J^2 - J)\delta}}{J} \left[m_4 (k_{HF} n_{HF} + k_F n_F) + m_5 k_{H_2} n_{H_2} \right] \right\} \qquad (29)$$

where the functions $m_2 \cdots m_5$, which are plotted in Fig. 1, are given by

$$m_2 = \tfrac{1}{6}(1 + 2e^{-2J\delta} + 3e^{-4J\delta}), \qquad m_3 = (1 + e^{2J\delta})(1 + e^{-4J\delta})$$
$$m_4 = \frac{e^{2J\delta} + e^{-2J\delta} + (4/3)}{m_3}, \qquad m_5 = \frac{e^{2J\delta} - e^{-2J\delta} - 2}{m_3} \qquad (30)$$

Using Eq. (23), we express A_2 in terms of the extent of reaction parameter

$$A_2 = k\rho^2 (n_F n_{H_2})_0 \left\{ (1 - \xi)(1 - \kappa_1 \xi) + \left(\frac{\xi + \kappa_2}{m_3} + m_5 \alpha \right) (1 - \kappa_1 \xi) \bar{k}_{H_2} \right.$$
$$\left. + \kappa_1 \left[\frac{m_2}{m_3} (\xi + \kappa_2) + m_4 \alpha \right] \left[(\xi + \kappa_2) \bar{k}_{HF} + (1 - \xi) \bar{k}_F \right] \right\} \qquad (31)$$

where

$$\kappa_2 = \left(\frac{n_{HF}}{n_F}\right)_0, \qquad \alpha = \frac{g}{g_r}\,\frac{e^{(J^2-J)\delta}}{J}\,\frac{1}{(n_F)_0} \tag{32}$$

and ratios of rate coefficients to that for the pumping reaction are

$$\bar{k}_{H_2} = \left(k_{H_2}/k\right), \qquad \bar{k}_F = (k_F/k), \qquad \bar{k}_{HF} = (k_{HF}/k) \tag{33}$$

These ratios of rates are shown as functions of temperature in Fig. 2.

Substitution of (27) and (31) into (3) yields the central result

$$\chi_{rad} = k\rho^2\left(n_F n_{H_2}\right)_0\left\{(m_1 - 1)(1 - \xi)(1 - \kappa_1\xi) - \left(\frac{\xi + \kappa_2}{m_3} + m_5\alpha\right)(1 - \kappa_1\xi)\bar{k}_{H_2}\right.$$
$$\left. - \kappa_1\left[\frac{m_2}{m_3}(\xi + \kappa_2) + m_4\alpha\right]\left[(\xi + \kappa_2)\bar{k}_{HF} + (1 - \xi)\bar{k}_F\right]\right\} \tag{34}$$

With J and a set of initial conditions specified, quantities on the righthand side are constant except the timelike parameter ξ. The deactivation terms, i.e., those involving $\bar{k}_{H_2}$, $\bar{k}_{HF}$, and $\bar{k}_F$, all diminish χ_{rad}. We define ξ_c as that value of ξ for which χ_{rad} is reduced to zero. Lasing cuts off at $\xi = \xi_c$, and the corresponding time, obtained from Eq. (24), is t_c.

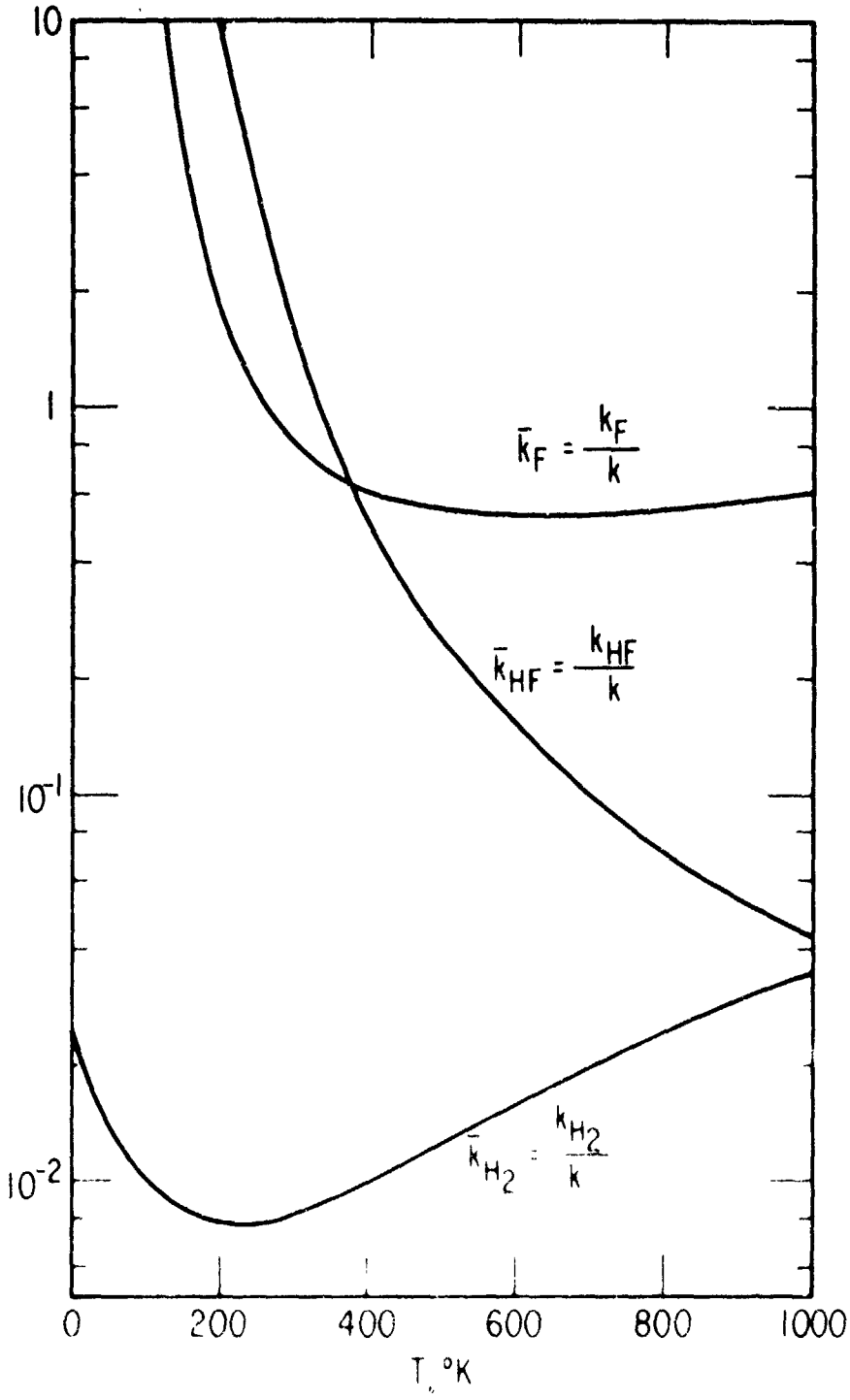

Figure 2. Rate Coefficient Ratios $\bar{k}_F$, $\bar{k}_{HF}$, and $\bar{k}_{H_2}$ vs Temperature

(See Table II for expressions for the rate coefficients.)

The time integral of χ_{rad} gives E and η, Eqs. (5) and (6). It is

$$\int_{t_0=0}^{t} \chi_{rad}\, dt = \frac{1}{k\rho\left(n_{H_2}\right)_0} \int_0^{\xi} \frac{\chi_{rad}(\xi)\, d\xi}{(1-\xi)(1-\kappa_1\xi)}$$

$$= \rho(n_F)_0 \Bigg\{ (m_1 - 1)\xi + \frac{\bar{k}_{H_2}}{m_3}[\xi + (1 + \kappa_2 + m_3 m_5 \alpha)\, \ell n(1-\xi)]$$

$$+ \frac{\bar{k}_F}{m_3}\left[m_2 \xi + \frac{(1+\kappa_1\kappa_2)m_2 + \kappa_1 m_3 m_4 \alpha}{\kappa_1}\, \ell n(1-\kappa_1\xi) \right]$$

$$+ \frac{\bar{k}_{HF}}{m_3}\left[-m_2\xi + \frac{\kappa_1(1+\kappa_2)[(1+\kappa_2)m_2 + m_3 m_4 \alpha]}{1-\kappa_1}\, \ell n(1-\xi) \right.$$

$$\left. - \frac{(1+\kappa_1\kappa_2)[(1+\kappa_1\kappa_2)m_2 + \kappa_1 m_3 m_4 \alpha]}{\kappa_1(1-\kappa)}\, \ell n(1-\kappa_1\xi) \right] \Bigg\} \tag{35}$$

As mentioned previously, J is chosen as that integer which maximizes η.

Simple scaling laws are superficially indicated by Eqs. (34) and (35) if one neglects, temporarily, the pressure-dependence of α. Output power is proportional to $k\rho^2\left(n_F n_{H_2}\right)_0$ and hence appears to scale as the pressure squared. Pulse energy is proportional to $\rho(n_F)_0$ and appears to scale linearly with the pressure. Efficiency appears to be independent of the pressure. It will be seen later that the pressure-dependence of α alters this simple scaling substantially.

For limiting cases, Eqs. (34) and (35) are simplified, and examination of certain features of the theory is facilitated.

A. THRESHOLD GAIN VANISHING

This is the case $g = 0$, which is approached as $L \to \infty$ or as $r_1 r_2 \to 1$. In Eqs. (34) and (35) we obtain this limit by setting $\alpha = 0$. Inspection of Eq. (34) shows that deactivation is less for $\alpha = 0$ than for finite α. Hence, as expected, best performance is predicted for the most effective cavity, i.e., for $g = 0$. With $\alpha = 0$, maximum efficiency occurs when $J \to \infty$, in accord with the analysis in Ref. 5. Later we shall find that whenever the α terms are nonzero maximum efficiency occurs at a finite J.

B. NO DEACTIVATION

In this limit $\bar{k}_{H_2} = \bar{k}_F = \bar{k}_{HF} = 0$ and the theory predicts

$$\chi_{rad} = k\rho^2 \left(n_F n_{H_2}\right)_0 (m_1 - 1)(1 - \xi)(1 - \kappa_1 \xi) \tag{36}$$

$$\xi_c = \begin{cases} 1/\kappa_1 & \text{for } \kappa_1 \geq 1 \\ 1 & \text{for } \kappa_1 < 1 \end{cases} \tag{37}$$

$$E(t) = 11.96\, \omega\rho (n_F)_0 (m_1 - 1)\xi \tag{38}$$

$$\eta = \frac{11.96 \times 10^2}{1.4 \times 10^5} \omega (m_1 - 1)\xi_c \tag{39}$$

Equation (37) predicts cutoff when n_F or n_{H_2} reaches zero and no further HF(v) can be formed. The intensity, which is proportional to χ_{rad}, decreases parabolically with ξ from its maximum value at $\xi = 0$. Maximum efficiency is achieved when m_1 has its maximum value of 3, and this occurs for $J \to \infty$.

Curiously, in this limiting case there is no dependence on g. This is caused by idealizations made in the development of Eq. (12) and also by neglect of the time interval of pumping needed to achieve threshold.

C. HYDROGEN-RICH MIXTURE

The case of a large excess of hydrogen with fixed fluorine is described by $\kappa_1 \to 0$, $(n_F)_0$ fixed. In this limit

$$\chi_{rad} \sim \frac{k\rho^2 (n_F)_0^2}{\kappa_1} \left[(m_1 - 1)(1 - \xi) - \left(\frac{\xi + \kappa_2}{m_3} + m_5 \alpha \right) \bar{k}_{H_2} \right] \tag{40}$$

$$\eta = 8.55 \times 10^{-3}\, \omega \left\{ (m_1 - 1)\xi + \frac{\bar{k}_{H_2}}{m_3} [\xi + (1 + \kappa_2 + m_3 m_5 \alpha)\, \ell n(1 - \xi)] \right\} \tag{41}$$

Fast pumping and deactivation by H_2 predominate. Because $\bar{k}_{H_2}$ is small in comparison with $\bar{k}_F$ and $\bar{k}_{HF}$ (see Fig. 2), a very small κ_1 is required for this limit to apply.

D. FLUORINE-LEAN MIXTURE

For $(n_F)_0 \to 0$, negative χ_{rad}'s are predicted. This, of course, is physically incorrect. In reality, when fluorine is very scarce, threshold, if achieved, is not achieved quickly. Thus, the theory is not suited to describing this limiting case, because the assumption $t_0 = 0$ is inappropriate.

The preceding limiting cases in part illustrate expected behavior and in part serve to point out regimes in which underlying assumptions of the theory are not fulfilled. On the basis of arguments similar to those for the fluorine-lean situation, we have found that the initial HF parameter κ_2 should be restricted to values small in comparison with unity for the theory to hold.

V. COMPARISON WITH COMPUTER MODEL

Development of this closed-form model for an F + H_2 laser was aided by simplifications suggested by study of computer modeling of the same laser. In this section, we compare predictions of our closed-form model with those of the more elaborate computer model. Basic features of each model were summarized earlier in Table I.

We consider cases in which the initial gas mixture has a composition with mole ratio SF_6:H_2:F:HF = 50:1:κ_1:$\kappa_1\kappa_2$ and a pressure of 20 Torr. A large amount of inert, high-heat-capacity diluent, SF_6, ensures a nearly isothermal gas condition. At 20 Torr, the transitions are largely Doppler-broadened. The length L is fixed at 10 cm, and the reflectivity r_2 is taken as 1.0. In anticipation of a parametric study over ranges of values for T, κ_1, κ_2, and r_1 to be presented later, we choose cases that provide a sampling of these ranges for comparison with the computer model.

Values for parameters in g_r, Eq. (9), and for ω appropriate for HF are:[5]

$$\sigma = 1, \qquad \Theta_r = 30.16^\circ K, \qquad W = 20 g/mol,$$

$$|\mathcal{M}|^2 = 2.8 \times 10^{-38} \text{ erg/cm}^3, \qquad \omega = 3790 \text{ cm}^{-1}.$$

Illustrations of the choice of a dominant J for the present theory are considered before we go on to the comparison with the computer model. To obtain a dominant J, we try several integer J values until a J giving maximum

η is found. Results of such a procedure are shown in Fig. 3. For each example the choice J = 7 gives maximum efficiency. Neighboring J's give moderately smaller efficiencies. Dominant J's were chosen in this way in all calculations.

Table III presents a comparison between the theory and computer modeling for four cases. In the table, t_0 is the time required for all three $v + 1 \rightarrow v$ transitions to reach threshold, T_c is the temperature at cutoff of lasing, and "output J" refers to values of J for transitions yielding the bulk of the output energy for all vibrational bands. The results for t_0 and T_c justify our assumptions of $t_0 = 0$ and isothermal conditions, respectively. The theory predicts values somewhat too large for the dominant J and the efficiency. However, the theory is accurate to within a factor of 1.3 for the efficiency for all cases.

On the basis of the results of Table III, the use in the theory of a single cutoff time appears to be questionable. Figure 4, which shows intensity vs time for Case A, demonstrates that the numerical calculations typically have a long, low-energy tail that can be disregarded. Thus, the large variation in cutoff times is not as serious as first appears. The overall agreement of pulse shape shown in Fig. 4 is quite good.

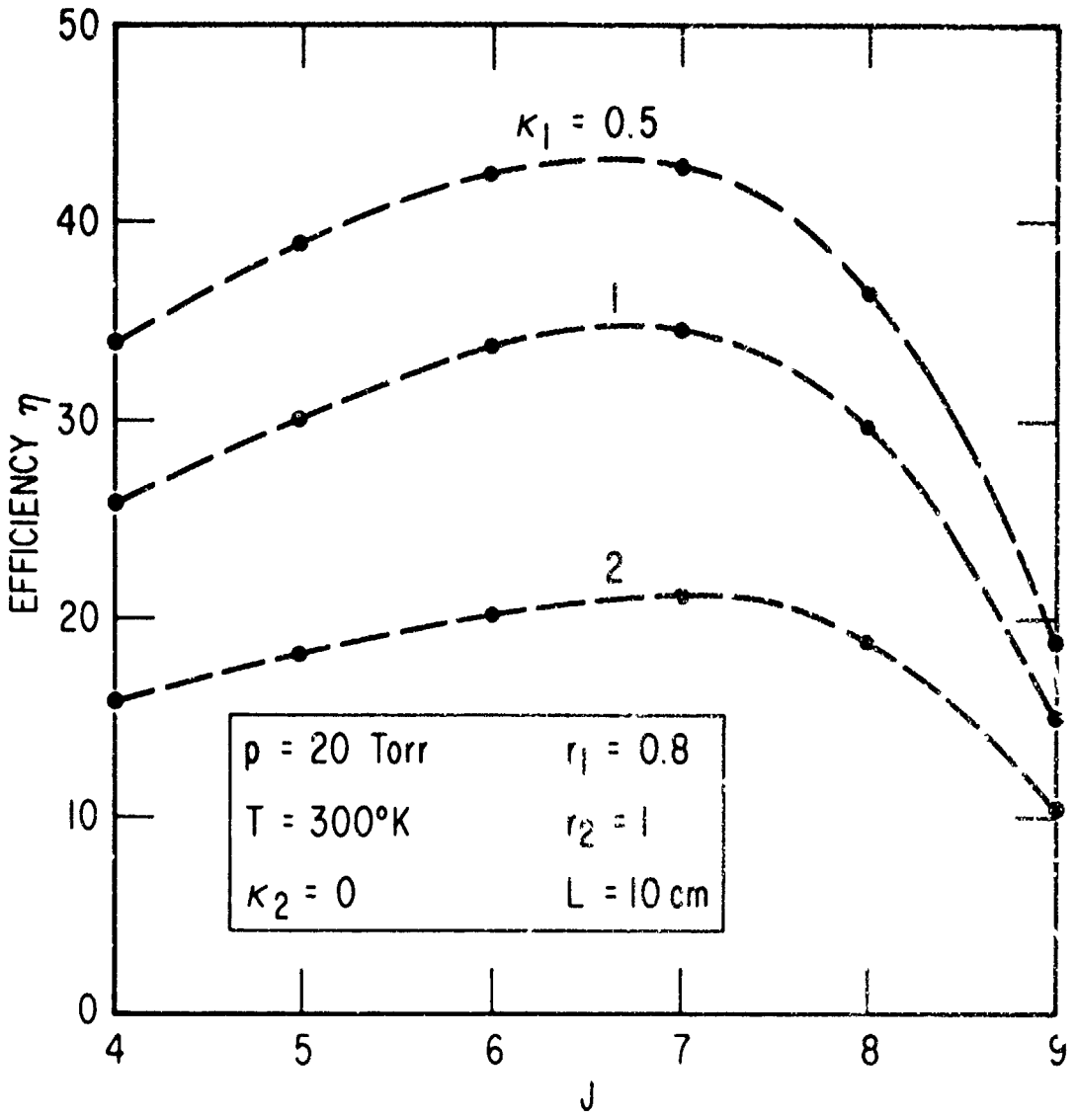

Figure 3. Efficiency vs Rotational Quantum Number J

(Maximum efficiency occurs for J = 7 for all three cases.)

Table III. Predictions of Theory Compared with Those of Computer Model

Specified Parameters	Case			
	A	B	C	D
T, °K	200	300	400	300
κ_1	0.5	1	2	1
κ_2	0	0	0	0.1
r_1	0.8	0.6	0.4	0.6
Computer Model Results				
t_0, μsec	0.12	0.14	0.20	0.54
(1 → 0) t_c, μsec	21.9	12.9	6.1	11.4
(2 → 1) t_c, μsec	36.1	18.5	7.2	16.8
(3 → 2) t_c, μsec	19.5	6.4	2.4	5.9
Output J	4, 5	4, 5, 6	5, 6	5, 6
T_c, °K	210	311	410	311
η	35.4	27.8	13.8	24.7
Results of Theory				
t_c, μsec	24.1	12.9	4.9	11.5
Dominant J	5	6	7	6
η	36.4	32.1	18.1	29.5

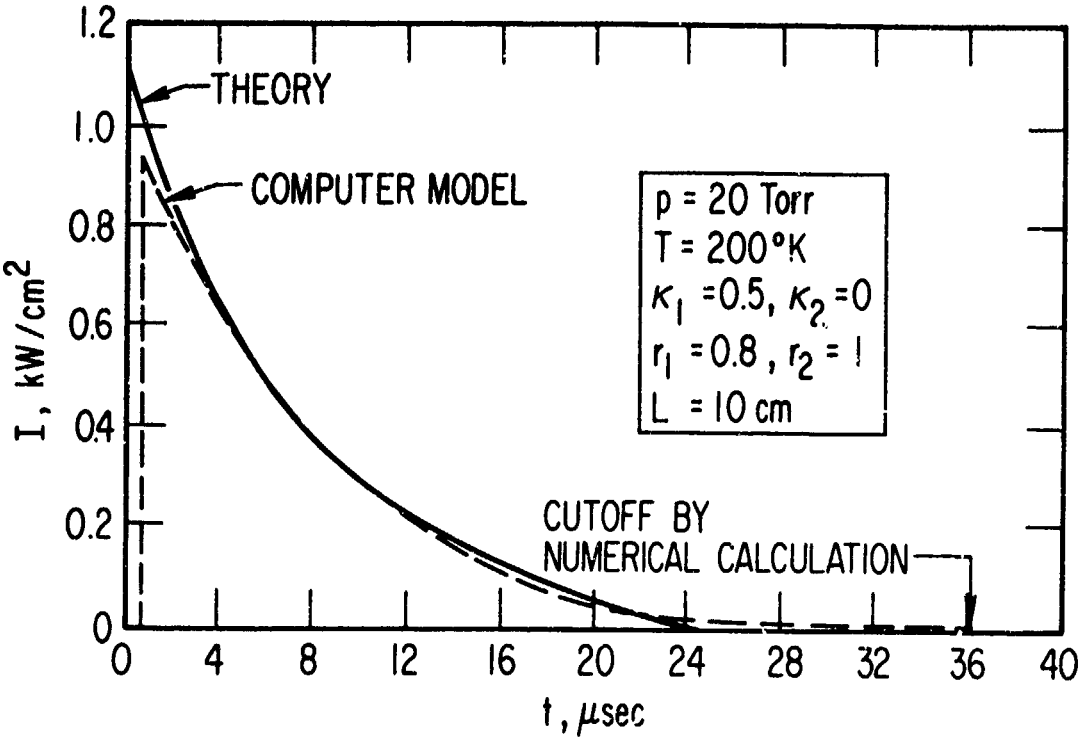

Figure 4. Output Intensity vs Time for Case A of Table III (Assumptions for the computer model are listed in Table I.)

VI. PARAMETRIC STUDY

The theory is used to study the dependence of laser performance on the parameters — pressure p, temperature T, initial fluorine-to-hydroden ratio κ_1, initial HF-to-fluorine ratio κ_2, and mirror reflectivity r_1 for fixed values of length L = 10 cm and reflectivity $r_2 = 1.0$. The relative importance of pumping and deactivation reaction rates is assessed with the aid of reaction rate parameters defined as follows:

$$d_p = (m_1 - 1)\xi \tag{42}$$

$$d_{H_2} = \frac{\bar{k}_{H_2}}{m_3}[\xi + (1 + \kappa_2 + m_3 m_5 \alpha)\, \ell n(1 - \xi)] \tag{43}$$

$$d_F = \frac{\bar{k}_F}{m_3}\left\{m_2\xi + \kappa_1^{-1}[(1 + \kappa_1\kappa_2)m_2 + \kappa_1 m_3 m_4 \alpha]\, \ell n(1 - \kappa_1\xi)\right\} \tag{44}$$

For d_{HF} the form depends on the value of κ_1. For $\kappa_1 \neq 1$

$$d_{HF}(\kappa_1 \neq 1) = \frac{\bar{k}_{HF}}{m_3}\Big\{-m_2\xi + (1 - \kappa_1)^{-1}\kappa_1(1 + \kappa_2) \times [(1 + \kappa_2)m_2 + m_3 m_4 \alpha]\, \ell n(1 - \xi) - \left(\kappa_1 - \kappa_1^2\right)^{-1}(1 + \kappa_1\kappa_2) \times [(1 + \kappa_1\kappa_2)m_2 + \kappa_1 m_3 m_4 \alpha]\, \ell n(1 - \kappa_1\xi)\Big\} \tag{45a}$$

and for $\kappa_1 = 1$

$$d_{HF}(\kappa_1 = 1) = \frac{\bar{k}_{HF}}{m_3}\left\{-m_2\xi - (1+\kappa_2)[m_2(1+\kappa_2) + m_3 m_4 \alpha]\frac{\xi}{1-\xi}\right. \tag{45b}$$

$$\left. - [2(1-\kappa_2^2)m_2 + m_3 m_4 \alpha]\, \ell n(1-\xi)\right\}$$

In terms of the d's, pulse energy and efficiency are given by

$$E(t) = 11.96\, \omega p (n_F)_0 \left(d_p + d_{H_2} + d_F + d_{HF}\right) \tag{46}$$

$$\eta = 8.55 \times 10^{-3}\, \omega \left(d_p + d_{H_2} + d_F + d_{HF}\right)_c \tag{47}$$

Thus, the d's allow us to assess the importance of the deactivation mechanisms relative to each other and to the pumping mechanism d_p.

Results of a parametric study for initial gas composition with mole ratio $SF_6:H_2:F\cdot HF = 50:1:\kappa_1:\kappa_1\kappa_2$ and p = 20 Torr are presented in Table IV for combinations of T = 200°K, 300°K, 400°K and r_1 = 0.8, 0.6, 0.4 for the cases $\kappa_1 = 0.5$, $\kappa_2 = 0$; $\kappa_1 = 1.0$, $\kappa_2 = 0$; $\kappa_1 = 2.0$, $\kappa_2 = 0$, and $\kappa_1 = 1.0$, $\kappa_2 = 0.1$.

Table IV shows that d_{H_2} is negligible in comparison with d_F and d_{HF}. This is consistent with the small values of $\bar{k}_{H_2}$ i comparison with those of $\bar{k}_F$ and $\bar{k}_{HF}$ in the temperature range of interest (see Fig. 2). Considering the main deactivators we see that, with few exceptions, d_{HF} is larger than d_F. However, when $\kappa_1 = 2$ and T = 300 and 400°K, excess fluorine and high temperature cause d_F to predominate. Throughout the table, increasing

Table IV. Parametric Study

T, °K	r_1	J	ξ_c	$t_{c,}$ μsec	d_p	$-d_{H_2}$	$-d_F$	$-d_{HF}$	E, J/cm^3	η
	$\epsilon_1 = 0.5$		$\epsilon_2 = 0$							
200	0.8	5	0.805	24 15	1.388	1.194^{-3}[a]	2.653^{-2}	2.370^{-1}	8.165^{-4}	36.39
	0.6	5	0.777	21.75	1.340	1.091^{-3}	3.410^{-2}	2.531^{-1}	7.641^{-4}	34.06
	0.4	5	0.741	19.14	1.278	9.847^{-4}	4.379^{-2}	2.677^{-1}	7.012^{-4}	31.25
300	0.8	7	0.917	15.84	1.550	2.752^{-3}	3.963^{-2}	1.814^{-1}	6.421^{-4}	42.92
	0.6	6	0.911	15.35	1.463	2.808^{-3}	3.743^{-2}	1.728^{-1}	6.053^{-4}	40.46
	0.4	6	0.887	13.51	1.424	2.546^{-3}	5.183^{-2}	1.954^{-1}	5.689^{-4}	38.03
400	0.8	8	0.949	13.41	1.523	4.885^{-3}	5.074^{-2}	1.322^{-1}	4.849^{-4}	43.22
	0.6	7	0.945	13.03	1.442	4.808^{-3}	4.966^{-2}	1.284^{-1}	4.573^{-4}	40.76
	0.4	7	0.924	11.27	1.410	4.280^{-3}	7.368^{-2}	1.531^{-1}	4.281^{-4}	38.16
	$\epsilon_1 = 1.0$		$\epsilon_2 = 0$							
200	0.8	6	0.622	17.78	1.124	4.497^{-4}	4.784^{-2}	2.194^{-1}	1.245^{-3}	27.74
	0.6	5	0.607	16.66	1.047	4.818^{-4}	4.339^{-2}	1.985^{-1}	1.169^{-3}	26.06
	0.4	5	0.582	15.01	1.004	4.480^{-4}	5.101^{-2}	2.040^{-1}	1.087^{-3}	24.23
300	0.8	7	0.767	13.90	1.296	1.156^{-3}	6.046^{-2}	1.681^{-1}	1.033^{-3}	34.52
	0.6	6	0.753	12.91	1.209	1.176^{-3}	5.880^{-2}	1.583^{-1}	9.598^{-4}	32.08
	0.4	6	0.729	11.40	1.171	1.092^{-3}	7.162^{-2}	1.662^{-1}	9.028^{-4}	30.18
400	0.8	8	0.815	12.63	1.307	2.013^{-3}	8.333^{-2}	1.321^{-1}	7.915^{-4}	35.28
	0.6	7	0.804	11.84	1.227	1.990^{-3}	8.234^{-2}	1.258^{-1}	7.387^{-4}	32.92
	0.4	7	0.776	9.99	1.184	1.799^{-3}	1.050^{-1}	1.336^{-1}	6.855^{-4}	30.55
	$\epsilon_1 = 2.0$		$\epsilon_2 = 0$							
200	0.8	6	0.399	11.79	0.721	1.380^{-4}	4.600^{-2}	1.091^{-1}	1.645^{-3}	18.33
	0.6	5	0.388	10.87	0.670	1.507^{-4}	4.308^{-2}	1.009^{-1}	1.528^{-3}	17.03
	0.4	5	0.377	10.04	6.506^{-1}	1.461^{-4}	4.870^{-2}	1.049^{-1}	1.444^{-3}	16.09
300	0.8	7	0.454	7.540	7.675^{-1}	2.526^{-4}	5.692^{-2}	5.970^{-2}	1.261^{-3}	21.07
	0.6	6	0.448	7.062	7.192^{-1}	2.654^{-4}	5.616^{-2}	5.802^{-2}	1.172^{-3}	19.58
	0.4	6	0.439	6.460	7.049^{-1}	2.613^{-4}	6.558^{-2}	6.276^{-2}	1.116^{-3}	18.66
400	0.8	8	0.464	5.780	7.447^{-1}	3.699^{-4}	7.190^{-2}	3.601^{-2}	9.247^{-4}	20.61
	0.6	7	0.460	5.490	7.016^{-1}	3.760^{-4}	7.139^{-2}	3.526^{-2}	8.639^{-4}	19.25
	0.4	7	0.449	4.880	6.856^{-1}	3.673^{-4}	8.727^{-2}	3.939^{-2}	8.116^{-4}	18.08
	$\epsilon_1 = 1.0$		$\epsilon_2 = 0.1$							
200	0.8	6	0.595	15.56	1.067	4.889^{-4}	4.794^{-2}	3.061^{-1}	1.035^{-3}	23.06
	0.6	5	0.571	14.36	9.851^{-1}	5.250^{-4}	4.462^{-2}	3.075^{-1}	9.190^{-4}	20.48
	0.4	5	0.545	12.95	9.410^{-1}	4.881^{-4}	5.113^{-2}	3.069^{-1}	8.464^{-4}	18.86
300	0.8	7	0.747	12.52	1.263	1.269^{-3}	6.199^{-2}	2.072^{-1}	9.617^{-4}	32.15
	0.6	6	0.732	11.54	1.174	1.294^{-3}	6.105^{-2}	2.023^{-1}	8.814^{-4}	29.46
	0.4	6	0.708	10.23	1.136	1.204^{-3}	7.277^{-2}	2.087^{-1}	8.264^{-4}	27.62
400	0.8	8	0.800	11.52	1.284	2.219^{-3}	8.516^{-2}	1.558^{-1}	7.561^{-4}	33.70
	0.6	7	0.788	10.74	1.203	2.202^{-3}	8.474^{-2}	1.512^{-1}	7.008^{-4}	31.23
	0.4	7	0.760	9.120	1.159	1.997^{-3}	1.060^{-1}	1.584^{-1}	6.486^{-4}	28.91

[a] Abbreviated notation for powers of 10 has been employed. Thus $1.194^{-3} = 1.194 \times 10^{-3}$, etc.

temperature causes d_{HF} to decrease in magnitude like the $\bar{k}_{HF}$ curve in Fig. 2.

Increasing r_1 causes moderate increases in η, ξ_c, and t_c. As r_1 increases the dominant J increases, as shown in Ref. 5. Here, however, the increase in J is never greater than one when r_1 varies between 0.4 and 0.8.

The effect of initial HF is shown by a comparison of the group of cases for $\kappa_1 = 1.0$, $\kappa_2 = 0.1$ with corresponding cases for $\kappa_1 = 1.0$, $\kappa_2 = 0$. In each case, initial HF causes a drop in efficiency; the effect is greatest for T = 200°K.

For most cases in Table IV the efficiency is largest when T = 400°K and smallest when T = 200°K. The differences, however, are less than might be anticipated from the $\bar{k}_{HF}$ and $\bar{k}_F$ curves in Fig. 2. Indeed, one might conclude, reasoning solely from those curves, that lasing could not occur at T = 200°K. However, even at 200°K and with initial HF present, i.e., $\kappa_2 = 0.1$, the deactivation processes are stronger but are not dominant. This conclusion stems from a comparison of $|d_{H_2} + d_F + d_{HF}|$ with dp.

An exception to the main trend with temperature is the group of cases for $\kappa_1 = 2.0$, $\kappa_2 = 0$, where the largest efficiencies are found at 300°K. The cause of this behavior is the change in temperature-dependence of the deactivation for this fluorine-rich case, in which d_F and d_{HF} are of nearl, equal importance.

These trends of efficiency vs temperature prompted us to investigate an extended range of temperature for the case $\kappa_1 = 1$, $\kappa_2 = 0$, $r_1 r_2 = 0.8$. For this case it was found that efficiency peaks at 400°K and decreases monotonically for higher temperatures.

Throughout the study we have found that the dominant J corresponds to the abscissa interval in Fig. 1 for which m_3 begins to rise steeply. The interval is indicated by vertical dashed lines in Fig. 1. Low temperatures favor the right side of the interval, high temperatures the left. Thus, larger deactivation at low temperature is, in part, countered by larger m_3, as shown by Eqs. (43)-(45) for the d's. These countervailing effects result in the existence of an optimum temperature for maximum efficiency. This m_3 effect is related to the temperature-dependence of the gain that makes molecular lasers most efficient at low rotational temperatures when deactivation processes are not considered.

The effect of an increase in the initial fluorine-to-hydrogen ratio κ_1 is shown by changes from group to group in the first three groups of data in Table IV. Efficiency is somewhat larger when H_2 is in excess, as shown by the $\kappa_1 = 0.5$ results. Decreased efficiency when $\kappa_1 = 2$ is caused by our fluorine-centered definition of efficiency, Eq. (6). We can obtain another view by examining trends of pulse energy and pulse duration with κ_1. For the case $T = 300°K$, $\kappa_2 = 0$, $r_1 r_2 = 0.8$, we have carried out calculations to supplement those of Table IV. Pulse energy increases with κ_1, rapidly at first, when there is excess H_2, and then more slowly for κ_1 greater than stoichiometric, where $\kappa_1 = 1$. Pulse duration, after a brief plateau for small κ_1, decreases monotonically. Shortening of the pulse with increasing κ_1 is to be expected because of the increased pumping rates.

Until now the examples have had a pressure of 20 Torr. The effect of changing the pressure is of interest, because at low enough pressures lasing

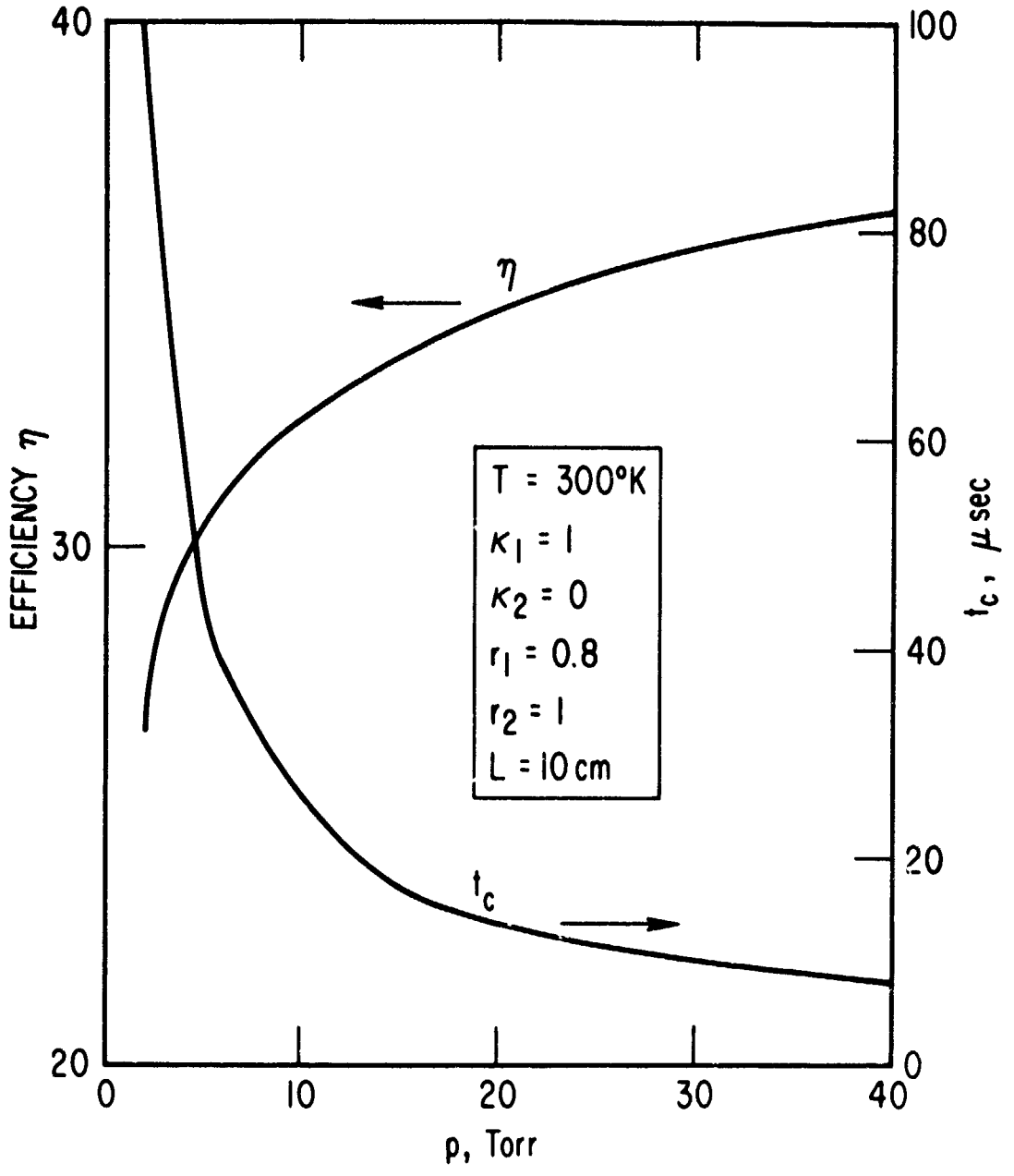

Figure 5. Efficiency and Pulse Length vs Pressure

VII. CONCLUSIONS

A theory providing a closed-form solution to rate equations for a chemically pumped, multilevel, molecular laser has been presented. Application is made to a pulsed HF laser pumped by the reaction $F + H_2 \rightarrow HF(v) + H$. Application to a cw laser is discussed in an appendix.

The analysis predicts laser intensity vs time, pulse energy, pulse duration, and efficiency. Because prediction of particular lasing transitions is avoided, spectral information is limited to prediction of a dominant J. Relative importance of pumping and deactivation rates is identified. To the approximation of a harmonic spacing of vibrational energy levels, it is found that laser performance predictions are independent of rate coefficients for HF - HF VV transfer. Good agreement is found in comparison of theoretical predictions with those of a comprehensive computer model for cases chosen to explore a wide range of parameters but restricted to avoid gross violations of the theoretical assumptions. A parametric study is presented that demonstrates the capability of the theory for economical prediction of a large number of trends.

Extension of the theoretical approach to other chemical systems seems desirable and feasible. The authors have obtained preliminary results for chain-reaction-pumped lasers. Extension of the theory for more detailed predictions of laser performance also appears possible but only at the expense of added complexity, which may prove to be uneconomical in comparison with computer modeling.

REFERENCES

1. J. R. Airey, J. Chem. Phys. 52, 156 (1970).
2. G. Emanuel, W. D. Adams, and E. B. Turner, "RESALE-1: A Chemical Laser Computer Program," TR-0172(2776)-1, The Aerospace Corporation, El Segundo, Calif., 1972.
3. R. L. Kerber, G. Emanuel, and J. S. Whittier, "Computer Modeling and Parametric Study for a Pulsed $H_2 + F_2$ Laser," TR-0172(2753)-3, The Aerospace Corporation, El Segundo, Calif., 1972; to be published in Appl. Opt., May 1972).
4. G. Emanuel, N. Cohen, and T. A. Jacobs, "Theoretical Performance of an HF Chemical CW Laser," TR-0172(2776)-2, The Aerospace Corporation, El Segundo, Calif., 1972.
5. G. Emanuel, "Analytical Model of a Continuous Chemical Laser," J. Quant. Spectr. Radiative Transf. 11, 1481 (1971).
6. W. C. Marlow, "Approximate Lasing Conditions," J. Appl. Phys. 41, 4019 (1970).
7. J. R. Airey and S. F. Fried, "Vibrational Relaxation of Hydrogen Fluoride," Chem. Phys. Letters 8, 23 (1971).

APPENDIX. APPLICATION TO CW LASERS

We consider a steady isothermal flow in the x direction with the laser cavity axis transverse to the flow, and we assume a Fabry-Perot cavity. With a flow of constant velocity u, the independent variable t of the pulse theory can be replaced with x/u. The equivalent to cumulative pulse energy, Eq. (5), in a flow system is the cumulative output power, in watts,[5]

$$P(t) = 11.96\,\omega(Au)\int_{t_0}^{t} \chi_{rad}\,dt$$

where A is the flow cross-sectional area and the integral is given by Eq. (35). Efficiency, Eq. (6), and intensity, Eq. (10), are unaltered.